Journal of Advanced Ceramics
2016, **5**(2): 167–175
DOI: 10.1007/s40145-016-0186-0

ISSN 2226-4108
CN 10-1154/TQ

Research Article

Preparation and characterisation of perovskite $La_{0.8}Sr_{0.2}Ga_{0.83}Mg_{0.17}O_{2.815}$ electrolyte using a poly(vinyl alcohol) polymeric method

Tong-Wei LI[a,*], Shu-Qiang YANG[b], Shuai LI[c,*]

[a]*School of Physics and Engineering*, *Henan University of Science and Technology*, *Luoyang 471023*, *China*
[b]*Department of Physics*, *Luoyang Normal University*, *Luoyang 471022*, *China*
[c]*Department of Energy Materials and Technology*, *General Research Institute for Nonferrous Metals*, *Beijing 100088*, *China*

Received: Feburary 18, 2016; Revised: March 08, 2016; Accepted: March 16, 2016

Abstract: The perovskite $La_{0.8}Sr_{0.2}Ga_{0.83}Mg_{0.17}O_{2.815}$ (LSGM) fuel cell electrolyte was prepared by a polymeric method using poly(vinyl alcohol) (PVA). The LSGM precursor powder was examined by thermogravimetric and differential thermal analysis (TG/DTA) and Fourier transform infrared (FTIR) spectroscopy. It was found that thermal decomposition of the LSGM precursor powder occurs in a number of different stages, and complete decomposition of the precursor is obtained at 1000 ℃. X-ray diffraction (XRD) showed that calcined powder contains three secondary phases, namely $La_4Ga_2O_9$, $LaSrGa_3O_7$, and $LaSrGaO_4$, even after calcination at 1100 ℃. Furthermore, the fraction of secondary phases decreases with increasing calcination temperature. Single phase perovskite LSGM pellets with a relative density of 97% were obtained after sintering at 1450 ℃ for 10 h. It was therefore shown that the powder prepared by the simple PVA method is fine, highly reactive, and sinterable. The electrical properties of LSGM pellets were characterised by impedance spectroscopy. The conductivity of the LSGM pellets sintered at 1450 ℃ for 10 h was 8.24×10^{-2} S/cm at 800 ℃.

Keywords: lanthanum gallate; perovskite; polymeric method; ionic conductivity

1 Introduction

The perovskite lanthanum gallate doped with Sr and Mg ($La_{1-x}Sr_xGa_{1-y}Mg_yO_{3-\delta}$, LSGM) has gained much attention in recent years for its high oxygen ionic conductivity at intermediate temperatures (500–800 ℃) [1–5]. In 1994, Ishihara *et al*. [2] studied the effect of different dopants on the electrical properties of perovskite $LaGaO_3$, and for the first time it was demonstrated that $LaGaO_3$ doped with Sr and Mg is a promising ionic conductor with its high conductivity. Feng and Goodenough [3] further reported that $La_{0.9}Sr_{0.1}Ga_{0.8}Mg_{0.20}O_{2.85}$ has an ionic conductivity $\sigma > 0.10$ S/cm at 800 ℃, and that the electrolyte is a pure oxygen ion conductor over a wide oxygen partial pressure range of 10^{-22} Pa $< p_{O_2} <$ 0.4 Pa. The chemical stability of the material was also tested and it was reported that the doped $LaGaO_3$ shows a stable performance over long operation time [2,5]. The electrical properties of LSGM ceramics with different compositions were investigated by Huang *et al.* [5]. The

* Corresponding authors.
E-mail: T.-W. Li, litjww@126.com; S. Li, shuaili04@gmail.com

highest ionic conductivity of $\sigma = 0.17$ S/cm was obtained for $La_{0.8}Sr_{0.2}Ga_{0.83}Mg_{0.17}O_{2.815}$ at 800 ℃. Thus the Sr- and Mg-doped $LaGaO_3$ is a promising material as an electrolyte in solid oxide fuel cells.

The $LaGaO_3$ based oxides are normally produced by solid state reaction [2–8]. Although the method is used for its simplicity, the process is not satisfactory due to drawbacks such as impurities introduced by milling, high reaction temperature, coarse grains, and low chemical homogeneity. Thus, wet chemical approaches are widely used to prepare the LSGM ceramics: sol–gel [9,10], Pechini [11–13], combustion [14], and hydrothermal [15]. Huang and Goodenough [10] successfully prepared $La_{0.8}Sr_{0.2}Ga_{0.83}Mg_{0.17}O_{2.815}$ powder by a coprecipitation method using ammonia to peptize an acetate solution of the cations. Ultrafine powder with nanosized particles was obtained after calcinations; however, the process needed expensive acetate salts and the reaction mechanism was difficult to control. The Pechini method is also used to synthesize LSGM ceramics [11]. This route involves the chelation process between citric acid and metal cations, and polymerization of these chelates [16]. As reported, the metal cations disperse uniformly at atomic level in the polymer network, which may ensure homogeneous and fine powder. In addition, the glycine nitrate combustion method and hydrothermal route have also been developed by Cong *et al*. [14] and Chen and Fung [15]. However, the phase purity and microstructure might strongly depend on the synthesis route, and the preparation of pure perovskite phase was rather difficult. It has been reported in various works that secondary phases such as $LaSrGa_3O_7$, $LaSrGaO_4$, or MgO are found after high temperature treatment of LSGM samples [11–14]. Taş *et al*. [11] further suggested that prolonged calcination time and increasing sintering temperature (e.g., 1470–1500 ℃) could remove these secondary phases. Nevertheless, a simple method to synthesize purer LSGM ceramics at lower temperatures is desirable.

The poly(vinyl alcohol) (PVA) polymeric route is an attractive method to prepare multicomponent oxides. According to Kriven *et al*. [17–19], the method mainly involves steric entrapment of metal cations in the polymer network, and thus offers a homogeneous dispersion of components. Ultrafine, homogeneous, and highly reactive oxide powder has successfully been prepared by using the PVA method. Phase pure LSGM pellets were obtained when this PVA method was investigated by Li *et al*. [20] and Zhai *et al*. [21]. Furthermore, the method does not need high temperatures. For example, the sintering temperature for the $La_{0.85}Sr_{0.15}Ga_{0.85}Mg_{0.15}O_{2.85}$ pellets prepared by PVA method was 50–100 ℃ lower, compared with the solid state method [20]. Although the method has been successfully applied to the preparation of LSGM ceramics, there is still a need for detailed investigation of the thermal decomposition process for the LSGM precursor powder prepared through this PVA method and the resulting electrical properties of sintered pellets. In this work, we report a systematic study on the preparation of LSGM ceramics by the PVA method. The calcined powder was characterised by thermogravimetric and differential thermal analysis (TG/DTA), Fourier transform infrared (FTIR) spectroscopy, and X-ray diffraction (XRD). We also measured and discussed the impedance spectra for the sintered LSGM pellets.

2 Experimental

2. 1 Material preparation

Nitrate salts were used for the synthesis of LSGM: $La(NO_3)_3{\cdot}6H_2O$ (99.99%), $Sr(NO_3)_2$ (99.97%), $Ga(NO_3)_3{\cdot}xH_2O$ (99.9%, x was determined to be 9 using thermogravimetric analysis), and $Mg(NO_3)_2{\cdot}6H_2O$ (99.97%) (Alfa Aesar). These nitrate salts were dissolved in distilled water in stoichiometric proportions and homogenized by stirring on a hot plate. To obtain the PVA solution, an appropriate amount of PVA ($-(CH_2-CHOH)-_n$, molecular weight of 57000–66000, Alfa Aesar) was added to distilled water, and stirred at 150 ℃ until completely dissolved. Then the prepared solutions were mixed in a glass beaker. The proportion of PVA to nitrate salts was adjusted in such a way that the ratio of positively charged valences from the metal cations to the hydroxyl groups from the PVA is 1.5:1. The precursor solution was homogenized for 1 h at room temperature, and then heated to 250 ℃ to evaporate water. No precipitation was observed as water evaporated. A foam-like aerogel was finally formed. The foam was formed from the NO_x gas evolved during the decomposition of nitrates [17]. The aerogel obtained was ground in an agate mortar, and then calcined over a temperature range of 250–1100 ℃ for 6 h.

To break up the agglomerates, the 1000 ℃ calcined powder was ball milled for 1 h using a planetary mill. ZrO_2 balls (diameter: 5 mm) were used as milling media,

and ethanol as solvent. The milled and dried powder was then uniaxially pressed into pellets with a compaction pressure of 200 MPa. Green pellets were sintered at temperatures in the range of 1350–1450 ℃ with a heating rate of 5 ℃/min.

2. 2 Characterisation

Phase evolution in the samples was investigated by means of powder X-ray diffraction (XRD) (X'Pert Pro, PANalytical) using Cu Kα radiation (45 kV, 40 mA). Scans were taken in the 2θ range of 20°–80° with a step size of 0.017°. Lattice parameters were evaluated from all the diffraction peaks, using the UNIT-CELL program [22].

The thermal decomposition process of the LSGM precursor powder was examined by thermogravimetric analysis (TG) (TAG 24, SETARAM) and differential thermal analysis (DTA) (TG-DTA 1600, Labsys). The powder was heated to 1200 ℃ with air flow at a heating rate of 10 ℃/min. Al_2O_3 powder was used as reference material in the DTA test.

Fourier transform infrared (FTIR) (IFS 55, Bruker) spectroscopy was performed to analyze the chemical structure in the calcined powder. Measurements were made in the range 400–4000 cm^{-1}. The powder was mixed with dry KBr to form pellets for the FTIR.

The impedance spectra of sintered pellets were measured by impedance spectroscopy (SI 1260 impedance/Gain-phase analyzer, Solartron). Sintered pellets were first wet-ground to a thickness of about 1 mm. Platinum paste (ChemPur) was applied on both sides of the pellets and cured at 1100 ℃ for 0.5 h. Impedence measurements were made on cooling from 800 to 250 ℃ at interval of 50 ℃ in the frequency range from 10 MHz to 0.1 Hz with an ac amplitude of 80 mV. The impedance spectrum was analyzed using the ZView 2 software. Impedance from cables, leads, and sample holders obtained by measuring a blank cell was subtracted from the sample impedance spectra.

3 Results and discussion

3. 1 Thermal analysis

The thermal decomposition behavior of the LSGM precursor powder prepared by the PVA method is characterised by TG and DTA, as shown in Fig. 1. The DTA curve exhibits a weak and broad endothermic peak

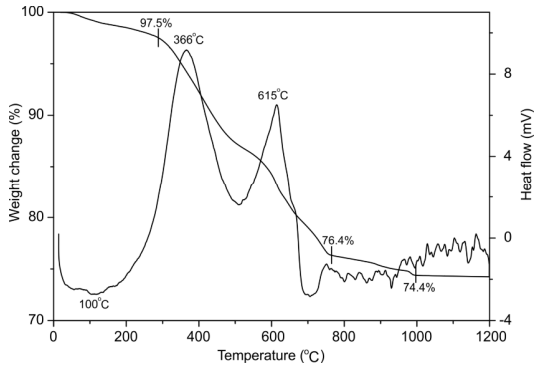

Fig. 1 TG/DTA curves showing the thermal decomposition of the LSGM precursor powder.

at around 100 ℃, which is followed by two pronounced exothermic peaks at 366 and 615 ℃. The TG curve shows the thermal weight loss as a function of temperature, corresponding to the DTA peaks. Clearly, most of the organics in the precursor powder decompose at temperatures < 760 ℃, yielding a weight loss of 23.6% (from the TG curve). Furthermore, the thermal decomposition can be divided into three stages as shown in Fig. 1. The first stage occurs below 290 ℃, with a weight loss of 2.5% related to the weak endothermic peak at 100 ℃. This weight loss is ascribed to the desorption of absorbed water. The PVA decomposes to polyenes and water through dehydration at the start of pyrolysis [18], so dehydration and depolymerisation of the polymeric residual from the precursor could be another reason for this weight loss. The second stage occurs in the temperature range of 290–760 ℃ with a weight loss of 21.1%, which is explained by the complex decomposition reactions of organics and nitrates. Carbonates, such as $SrCO_3$ or $MgCO_3$, are also believed to be present at this stage. In the third stage, at temperatures in the range of 760–1000 ℃, a slight 2.0% weight loss is observed. This weight loss could be due to the decomposition of carbonate intermediates [18,21]. There is no evidence of additional weight loss above 1000 ℃, which indicates the LSGM precursor powder has completely decomposed. The small peaks shown in the DTA curve above 800 ℃ are believed to be the background noise.

3. 2 IR spectra

The chemical structure of the calcined LSGM powder is further examined by FTIR. Figure 2 shows the FTIR spectra for the powder heated between 250 and 1100 ℃. The spectrum for the 250 ℃ calcined powder exhibits

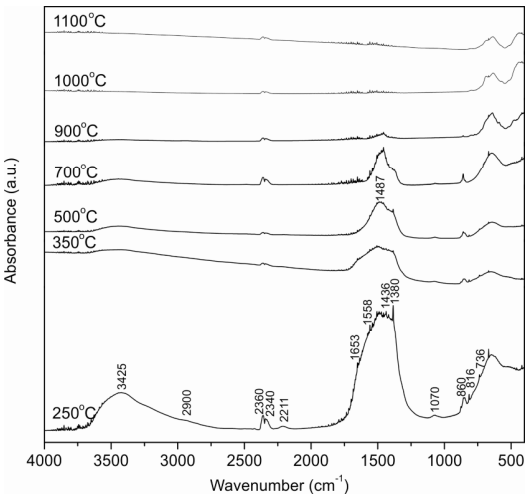

Fig. 2 FTIR spectra of LSGM powder calcined at different temperatures.

extensive absorption peaks, as shown in Fig. 2. The broad band at 3200–3600 cm^{-1} is due to O–H stretching vibration. The presence of $–CH_2$ groups is detected by a weak broad band at 2900 cm^{-1}, which is assigned to C–H stretching vibration. The weak peak at 2211 cm^{-1} may indicate the presence of C≡C in the 250 ℃ calcined powder; the peak disappears with increasing temperature. As mentioned above, PVA dehydrates to polyenes during pyrolysis, and the presence of these polyenes is indicated by the medium bands located at 1653 cm^{-1} (stretching vibration of C=C) and 816 cm^{-1} (bending of C–H). Double bands, produced by acetate groups, are observed at 1558 cm^{-1} (asymmetrically stretching vibration of COO^-) and 1436 cm^{-1} (symmetrically stretching vibration of COO^-) [10]. Remaining nitrate salts in the LSGM powder are also found with the bands from NO_3^-, located at 1380 cm^{-1} (asymmetrically stretching vibration) and 736 cm^{-1} (in plane bending). In addition, the medium bands at 1070 and 860 cm^{-1} can be attributed to the stretching vibration of CO_3^{2-}, which confirms the carbonates generated by the decomposition of organics and nitrates from the above thermal analysis. Moreover, there are two peaks located at 2360 and 2340 cm^{-1} that can not be identified. They may come from the atmospheric CO_2 according to the literature [11].

With increasing temperature, the FTIR spectra show significant changes in the C=C and NO_3^- bands, while only a slight decrease of the O–H band is observed. At 500 ℃, the band at 1653 cm^{-1} for C=C disappears in the powder, indicating that the polyene has decomposed at this stage. The band at 1487 cm^{-1} is due to the stretching vibration of CO_3^{2-}, which shows carbonate salts still remain in the powder. Further increase in temperature to 700 ℃ shows an apparent decrease of the NO_3^- band intensity, and the residual nitrate salts gradually decompose as temperature increases. The 900 ℃ calcined powder shows traceable vibrations from carbonates, and most organics vanish. The powder calcined at above 1000 ℃ has low frequency bands in addition to bands from CO_2. These low frequency bands are characteristic of metal-oxygen vibrations, which indicates a complete decomposition of the precursor powder has occurred, consistent with the result in Fig. 1.

3.3 Phase analysis

Figure 3 shows the XRD patterns for LSGM powder calcined at various temperatures. The XRD spectrum for the powder calcined at 250 ℃ has a broad arc-shaped continuum over 2θ range of 25°–30°. This indicates that the powder is mainly amorphous. The FTIR results show that nitrates and carbonates exist in powder calcined in the temperature range of 250–900 ℃, and this finding is also observed in XRD patterns. The two weak diffraction peaks of the 250 ℃ calcined powder are indexed as $Sr(NO_3)_2$ (JCPDS No. 25-0746). With increasing calcination temperature to 500 ℃, no significant change is observed for the XRD spectrum, and there is still a trace amount of $Sr(NO_3)_2$ in the amorphous powder, with no evidence of other crystalline phases. The powder consists of an

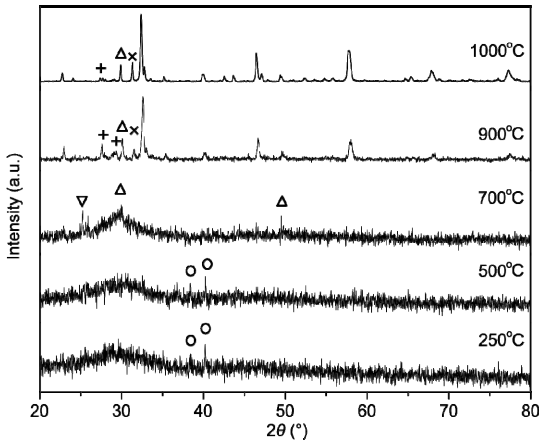

Fig. 3 XRD patterns showing phase evolution for the calcined LSGM powder: (○) $Sr(NO_3)_2$, (▽) $SrCO_3$, (Δ) $LaSrGa_3O_7$, (+) $La_4Ga_2O_9$, (×) $LaSrGaO_4$.

amorphous phase after calcination at 700 ℃; however, no $Sr(NO_3)_2$ is found but weak peaks from $SrCO_3$ (JCPDS No. 05-0418) and $LaSrGa_3O_7$ (JCPDS No. 45-0637) are seen. The nitrate salts vanish as the calcining temperature increases, corresponding well with FTIR. At 900 ℃, fully crystallized powder is formed since the arc-shaped continuum has completely disappeared from the XRD pattern. Furthermore, strong diffraction peaks from perovskite $LaGaO_3$ are observed, which means that perovskite $LaGaO_3$ phase is essentially formed after calcination at 900 ℃. Thus, it can be concluded that the formation of $LaGaO_3$ occurs through intermediate stages and not directly from the amorphous precursor.

The secondary phases in calcined powder are seen in the XRD patterns in Fig. 3. These secondary phases are identified as $La_4Ga_2O_9$ (JCPDS No. 53-1108), $LaSrGa_3O_7$ (JCPDS No. 45-0637), and $LaSrGaO_4$ (JCPDS No. 24-1208). All calcined powder has secondary phases, and the LSGM powder could not be obtained as phase pure even after calcination at 1100 ℃. The fraction of secondary phases is estimated by calculating the ratio of the integrated intensity of the most intense peaks of the secondary phases to the perovskite $LaGaO_3$ peak intensity. The fractions of secondary phases are estimated to be 42.8%, 36.1%, and 31.0% in powder calcined at 900, 1000, and 1100 ℃, respectively. Therefore, it can be concluded that these secondary phases decrease with increasing calcination temperature, as reported in previous works [13,20].

The phases in the sintered pellets were examined by XRD on the polished surface, as shown in Fig. 4. The pure perovskite $LaGaO_3$ phase could be obtained after sintering at 1450 ℃ for 10 h. All sintered pellets show cubic perovskite $LaGaO_3$ (JCPDS No. 24-1102). The diffraction data for the LSGM pellets sintered at 1450 ℃ for 10 h are given in Table 1. The lattice parameter obtained for the pellets is calculated to be a = 3.9077 Å. The secondary phases, namely $LaSrGa_3O_7$ and $LaSrGaO_4$, can still be detected in sintered pellets. However, the $La_4Ga_2O_9$ present in the calcined powder is eliminated by the sintering process. The fraction of secondary phases in sintered pellets, estimated from the XRD pattern, is shown in Table 2. The increasing temperature could apparently promote the dissolution of secondary phases in the sintered pellets. In addition, prolonged sintering time can also decrease the fraction of secondary phases, as shown in Table 2. LSGM pellets

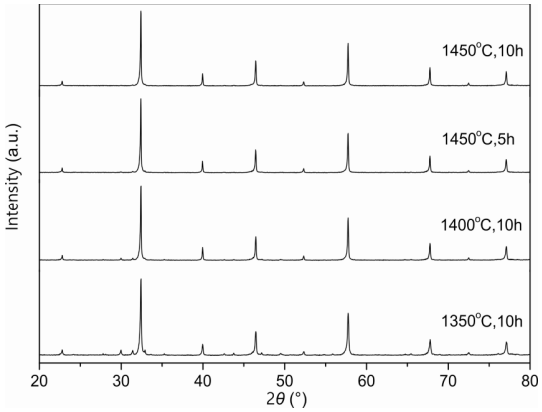

Fig. 4 XRD patterns for sintered LSGM pellets.

Table 1 XRD diffraction data of LSGM pellets sintered at 1450 ℃ for 10 h

2θ (°)	d (Å)	I/I_0	hkl
22.781	3.9003	6	1 0 0
32.407	2.7604	100	1 1 0
39.965	2.2540	16	1 1 1
46.448	1.9534	33	2 0 0
52.320	1.7471	5	2 1 0
57.752	1.5951	56	2 1 1
67.763	1.3817	24	2 2 0
72.477	1.3030	3	3 0 0
77.098	1.2360	19	3 1 0

Table 2 Estimation of the fraction of secondary phases and density of LSGM pellets

Specimen	$LaSrGa_3O_7$	$LaSrGaO_4$	Total	Density (g/cm^3)
1350 ℃, 10 h	5.6%	5.2%	10.8%	6.39
1400 ℃, 10 h	2.3%	2.3%	4.6%	6.37
1450 ℃, 5 h	0.6%	1.1%	1.7%	6.38
1450 ℃, 10 h	0	0	0	6.37

were prepared phase pure after sintering at 1450 ℃ for 10 h. Although the formation of single phase $LaGaO_3$ can also be obtained using the solid state reaction method, this usually needs a higher sintering temperature (e.g., > 1500 ℃) and much longer duration [5,23]. Compared with this traditional ceramic method, the sintering temperature for powder prepared by the PVA method is reduced by at least 50 ℃. Synthesis of single phase perovskite has been a basic requirement for $LaGaO_3$ based oxides, but lowering the sintering temperature is also desirable. A high sintering temperature may result in severe coarsening of grains and potential Ga evaporation. Stevenson *et al*. [24] have previously demonstrated that Ga evaporation in the form of Ga_2O could occur for LSGM sintered at 1500 ℃.

The density of sintered pellets, measured using Archimedes' method, is shown in Table 2. The

theoretical density of LSGM is calculated to be 6.56 g/cm^3 using the lattice parameter 3.9077 Å. The LSGM pellets sintered at 1450 ℃ for 10 h has a high relative density of 97%, showing that the LSGM powder prepared by the PVA method has a high sinterability. Therefore, it can be concluded that the PVA method can prepare phase pure and high density LSGM ceramics at a lower sintering temperature.

3. 4 Impedance spectra

Impedance spectroscopy was used to characterise the electrical properties of sintered LSGM pellets. The impedance spectrum normally separates bulk, grain boundary, and electrode processes of the ceramics. The high frequency semicircle in the impedance complex plane comes from the bulk conduction and dielectric process; the intermediate frequency semicircle is due to the grain boundary response, and the low frequency arc is attributed to electrode processes [6,8,9]. The impedance data can be analyzed by a simple hand fitting process [6], while a more quantitative approach uses an electrical equivalent circuit to model the spectrum and extract parameters [8]. Abram *et al*. [8] compared various equivalent circuits to model the impedance response of the LSGM ceramic. It was suggested that a suitable equivalent circuit is necessary in order to obtain parameters with physical significance. In the present work, the equivalent circuit approach was used to analyze the impedance spectrum of the sintered pellets.

Figure 5 shows the typical impedance spectrum for the LSGM pellets made by the PVA method. The spectrum has two semicircles, and they correspond to bulk and grain boundary responses. In addition, it is found that the bulk semicircle is slightly depressed, which means a constant phase element (CPE) existing parallel to R_b (a bulk resistor) and C_b (a bulk capacitor). The CPE can be written as follows:

$$Z_{CPE} = [Q_0(j\omega)^n]^{-1}$$

where Q_0 is a constant, n is the depressed exponent, and ω is the angular frequency. As shown in Fig. 5, the grain boundary semicircle for LSGM pellets is perfect, and thus consists of a parallel R_{gb} (grain boundary resistor) and C_{gb} (grain boundary capacitor) circuit. The equivalent circuit, given in Fig. 5, is used to fit the impedance data of LSGM pellets. In addition, corresponding complex formalisms are used to check the fitting parameters: impedance, modulus, admittance, and permittivity.

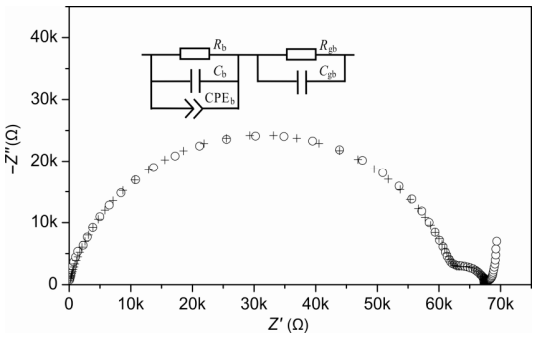

Fig. 5 Impedance spectrum for the LSGM pellets sintered at 1450 ℃ for 10 h measured at 250 ℃, and the equivalent circuit for impedance spectrum (open circle for the observed impedance data, and cross for the fitting data from the equivalent circuit) .

The fitting data for the impedance spectroscopy data are given in Fig. 5. Clearly, the equivalent circuit gives a good fit. This is further proved by Fig. 6, where fitting data provide a satisfactorily model for the real and imaginary parts of the four formalisms over the frequency range. The fitted values are R_b = 62.9 kΩ, $C_b = 5.2$ pF, $Q_0 = 3.65\times10^{-10}$ S·s^n and $n = 0.81$ for CPE, $R_{gb} = 4.4$ kΩ, $C_{gb} = 108$ nF.

The depressed exponent of CPE is 0.81 for the pellets measured at 250 ℃ (Fig. 5). For an R–C combination CPE, the value of n is $0 \leqslant n \leqslant 1$ [6]. The CPE represents a resistor for $n = 0$, and a capacitor for $n = 1$. Thus, the closeness of n to 1 in the LSGM pellets may indicate a greater capacitance component in the grain bulk. The depressed exponent for CPE is believed to be dependent on the secondary phases in LSGM pellets [6]. However, a more common explanation for CPE is the distortion introduced by local inhomogeneities [25]. In general, the microscopic properties are often distributed, for example, the ceramic contains two- or three-phase regions, local charge inhomogeneity, and variations in composition and stoichiometry. The capacitance and CPE depressed exponent for the pellets measured at different temperatures were also estimated. They were found to be insensitive to the measuring temperature, in good agreement with previous reports [6,8].

Figure 7 illustrates the change of the impedance spectrum with measurement temperature for the LSGM pellets sintered at 1450 ℃ for 10 h. At 350 ℃, the impedance spectrum can be resolved into two semicircles, corresponding to the bulk and grain boundary responses. When the temperature is increased to 400 ℃, the two semicircles still exist; however, the

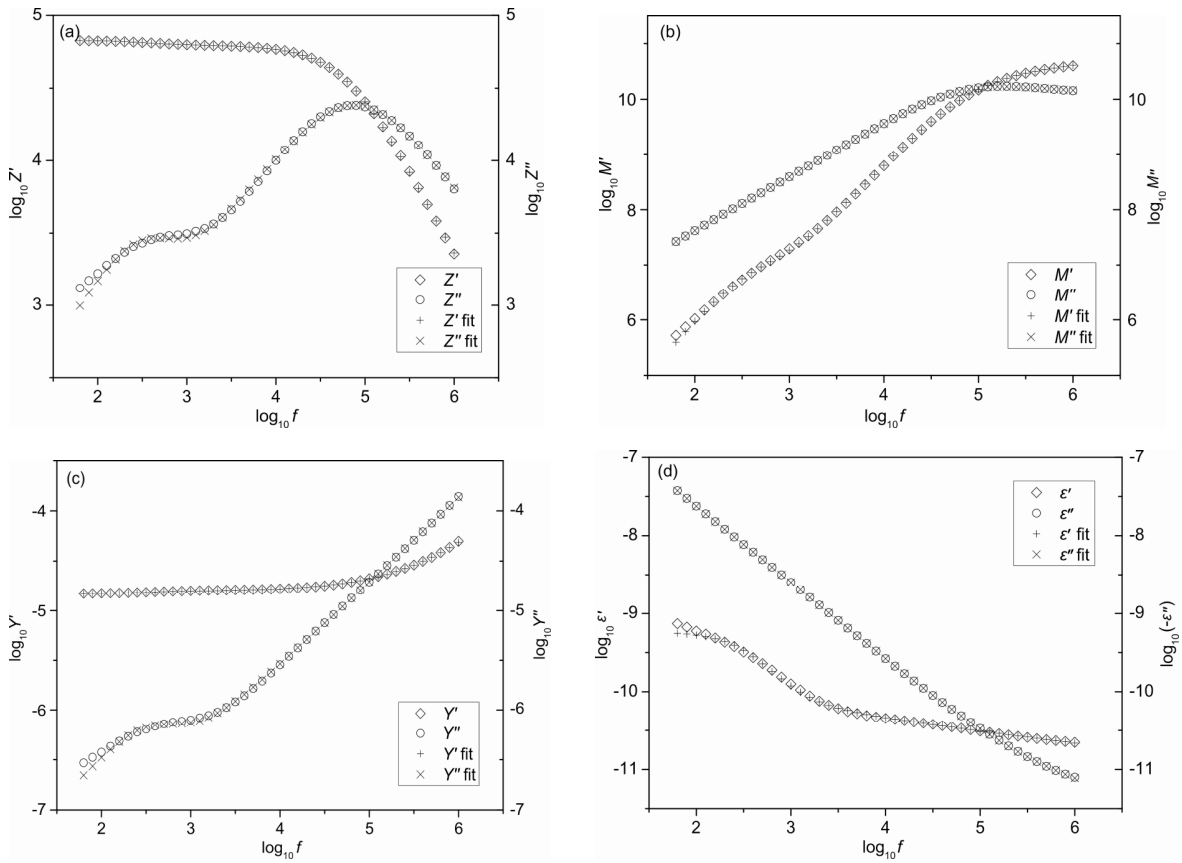

Fig. 6 Spectroscopic plots of the real and imaginary parts of (a) impedance *Z*, (b) modulus *M*, (c) admittance *Y*, (d) relative permittivity ε, and the fitted plots from equivalent circuit.

frequency limits are found to move to the higher end, as illustrated in Fig. 7. Further increase in temperature to 500 ℃ results in the total disappearance of the bulk semicircle in the spectrum. The resistance (*R*) and capacitance (*C*) follow the relationship $\omega_{\max}RC=1$, where $\omega_{\max}=2\pi f_{\max}$ is the angular frequency at the semicircle maximum. For temperatures $\geqslant$ 450 ℃, the dielectric relaxation time $\tau=RC$ becomes too small ($\tau<10^{-8}$) for $\omega_{\max}$ to fall within the high frequency limit. Only the electrode process arc can be detected in the impedance spectrum when the measurement temperature is higher than 600 ℃. Therefore, for temperatures higher than 600 ℃, the intercept between the real axis and spectrum is taken as the total resistance for the pellet.

3. 5 Conductivity

The temperature dependence of conductivity is shown in Fig. 8. The pellets sintered at 1450 ℃ for 10 h have the highest conductivity over all the measured temperature range, while inferior performance is demonstrated for the pellets sintered at 1400 ℃ for 10 h.

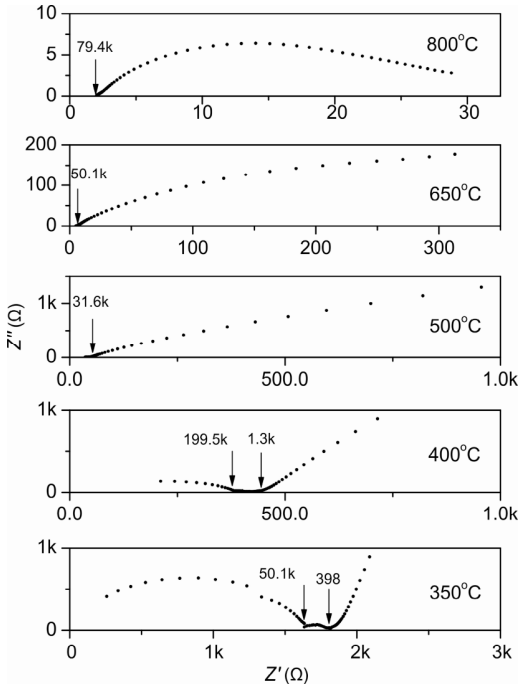

Fig. 7 Impedance spectra for the LSGM pellets sintered at 1450 ℃ for 10 h, measured at 350–800 ℃ (the arrow in the spectrum indicates the measuring frequency in Hz for the point).

Porosity may hinder oxygen ion migration and reduce the conductivity. However, porosity is not thought to be the reason for the low conductivity measured, since the sintered pellets have a relative density higher than 97%, as shown in Table 2. It is thought that secondary phases in the pellets exert a negative effect on the electrical conductivity. The fraction of secondary phases decreases with increasing sintering temperature or prolonged sintering time (Table 2). The secondary phases identified $LaSrGa_3O_7$ and $LaSrGaO_4$, have low ionic conductivity, and thus block oxygen ion migration [6]. The phase pure LSGM pellets sintered at 1450 ℃ for 10 h have the highest total conductivity of 0.08 S/cm.

The dependence of conductivity on temperature in the electrolyte can be expressed by the Arrhenius equation:

$$\sigma T = A\exp\left(-\frac{E}{kT}\right)$$

where A is a pre-exponential factor and E is the activation energy. It is observed in Fig. 8 that the curvature for the curve changes at 600 ℃. Feng and Goodenough [3] reported a similar phenomenon in $La_{0.9}Sr_{0.1}Ga_{0.8}Mg_{0.2}O_{3-\delta}$, which they attributed to the order–disorder transition associated with short range ordering of the oxygen vacancies around 600 ℃. An alternative explanation in another work attributed the effect to dopants, such as Sr and Mg, for isolated oxygen vacancies [5]. Dopants act as nucleation centers for the formation of ordered-vacancy clusters below the critical temperature T^*, while above this temperature the clusters dissolve into the oxygen sites. As shown in Fig. 8, the plotted curves are straight lines and parallel to each other over the temperature range 250–550 ℃, which indicates a similar activation energy (in this temperature range). However, there is apparent difference between the high temperature (600–800 ℃) curves, suggesting a different activation energy. The activation energies calculated are shown in Table 3. The Arrhenius plots of LSGM sintered at 1450 ℃ for 10 h give an activation energy of 1.078 eV in the temperature range 250–550 ℃, which compares well with the literature value of 1.07 eV [3,5].

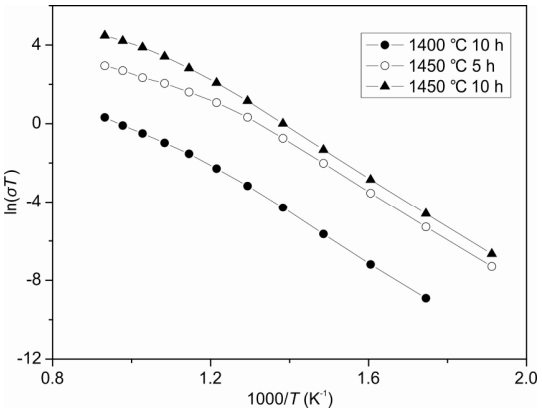

Fig. 8 Arrhenius plots of total conductivity for LSGM sintered pellets.

4 Conclusions

Single phase LSGM ceramics can be prepared by the PVA polymeric method. The thermal analysis (TG/DTA) shows that the decomposition of the LSGM precursor powder occurs in several stages. Desorption of water and depolymerisation of residual polymer in the precursor powder take place below 290 ℃. The complex decomposition of the polymer, nitrates, and carbonates occurs in the temperature range of 290–760 ℃. FTIR and XRD analysis further demonstrate the presence of nitrates and carbonates at this stage. The elimination of residual carbonates in the powder is completed in the range of 760–1000 ℃. Furthermore, XRD analysis shows that the $LaGaO_3$ phase forms at a calcination temperature of 900 ℃. Three secondary phases are detected in the calcined LSGM powders, namely $La_4Ga_2O_9$, $LaSrGa_3O_7$, and $LaSrGaO_4$; the fraction of these secondary phases depends on the calcination temperature. Higher sintering temperatures or longer sintering time further decrease the fraction of secondary phases. Phase pure and high density LSGM can be obtained by sintering at 1450 ℃ for 10 h. Impedance spectroscopy reveals a depressed grain bulk semicircle for LSGM pellets, indicating the presence of constant phase element (CPE) in the grains. The CPE is believed to be related to the distortion introduced by local inhomogeneities in sintered LSGM. A high conductivity,

Table 3 Total conductivity and activation energy for different LSGM pellets

Specimen	σ (S/cm)			lnA_1	E_1 (eV)	lnA_2	E_2 (eV)
	600 ℃	700 ℃	800 ℃				
1400 ℃,10 h	2.47×10^{-4}	6.23×10^{-4}	1.28×10^{-3}	13.12	1.090	8.35	0.744
1450 ℃, 5 h	5.71×10^{-3}	1.06×10^{-2}	1.78×10^{-2}	16.38	1.070	9.11	0.568
1450 ℃,10 h	1.92×10^{-2}	4.99×10^{-2}	8.24×10^{-2}	17.26	1.078	11.81	0.672

* lnA_1 and E_1 are calculated in the temperature range of 250–550 ℃.
** lnA_2 and E_2 are calculated in the temperature range of 600–800 ℃.

$\sigma = 8.24\times10^{-2}$ S/cm at 800 ℃, is obtained for the phase pure LSGM pellets sintered at 1450 ℃ for 10 h.

Acknowledgements

The authors would like to thank Prof. Zhicheng Li from the School of Materials Science and Engineering at Central South University (Hunan, China) for the helpful discussions and suggestions on this work. This work is supported by the Key Project for Education Department of Henan Province (Grant No. 16A140008), and the Innovation Team of Henan University of Science and Technology (Grant No. 2015XTD001).

References

[1] Fergus JW. Electrolytes for solid oxide fuel cells. *J Power Sources* 2006, **162**: 30–40.
[2] Ishihara T, Matsuda H, Takita Y. Doped $LaGaO_3$ perovskite type oxide as a new oxide ionic conductor. *J Am Chem Soc* 1994, **116**: 3801–3803.
[3] Feng M, Goodenough JB. A superior oxide-ion electrolyte. *Eur J Solid State Inorg Chem* 1994, **31**: 663–672.
[4] Huang P, Petric A. Superior oxygen ion conductivity of lanthanum gallate doped with strontium and magnesium. *J Electrochem Soc* 1996, **143**: 1644–1648.
[5] Huang K, Tichy RS, Goodenough JB. Superior perovskite oxide-ion conductor; strontium- and magnesium-doped $LaGaO_3$: I, phase relationships and electrical properties. *J Am Ceram Soc* 1998, **81**: 2565–2575.
[6] Huang K, Tichy RS, Goodenough JB. Superior perovskite oxide-ion conductor; strontium- and magnesium-doped $LaGaO_3$: II, ac impedance spectroscopy. *J Am Ceram Soc* 1998, **81**: 2576–2580.
[7] Djurado E, Labeau M. Second phases in doped lanthanum gallate perovskites. *J Eur Ceram Soc* 1998, **18**: 1397–1404.
[8] Abram EJ, Sinclair DC, West AR. A strategy for analysis and modelling of impedance spectroscopy data of electroceramics: Doped lanthanum gallate. *J Electroceram* 2003, **10**: 165–177.
[9] Huang K, Feng M, Goodenough JB. Sol–gel synthesis of a new oxide-ion conductor Sr- and Mg-doped $LaGaO_3$ perovskite. *J Am Ceram Soc* 1996, **79**: 1100–1104.
[10] Huang K, Goodenough JB. Wet chemical synthesis of Sr- and Mg-doped $LaGaO_3$, a perovskite-type oxide-ion conductor. *J Solid State Chem* 1998, **136**: 274–283.
[11] Taş AC, Majewski PJ, Aldinger F. Chemical preparation of pure and strontium- and/or magnesium-doped lanthanum gallate powders. *J Am Ceram Soc* 2000, **83**: 2954–2960.
[12] Polini R, Pamio A, Traversa E. Effect of synthetic route on sintering behaviour, phase purity and conductivity of Sr- and Mg-doped $LaGaO_3$ perovskites. *J Eur Ceram Soc* 2004, **24**: 1365–1370.
[13] Majewski P, Rozumek M, Tas AC, *et al*. Processing of $(La,Sr)(Ga,Mg)O_3$ solid electrolyte. *J Electroceram* 2002, **8**: 65–73.
[14] Cong L, He T, Ji Y, *et al*. Synthesis and characterization of IT-electrolyte with perovskite structure $La_{0.8}Sr_{0.2}Ga_{0.85}Mg_{0.15}O_{3-\delta}$ by glycine–nitrate combustion method. *J Alloys Compd* 2003, **348**: 325–331.
[15] Chen T-Y, Fung K-Z. Synthesis of and densification of oxygen-conducting $La_{0.8}Sr_{0.2}Ga_{0.8}Mg_{0.2}O_{2.8}$ nano powder prepared from a low temperature hydrothermal urea precipitation process. *J Eur Ceram Soc* 2008, **28**: 803–810.
[16] Pechini MP. Method of preparing lead and alkaline earth titanates and niobates and coating method using the same to form a capacitor. US Patent No. 3 330 697, 1967.
[17] Lee S-J, Kriven WM. Crystallization and densification of nano-size amorphous cordierite powder prepared by a PVA solution-polymerization route. *J Am Ceram Soc* 1998, **81**: 2605–2612.
[18] Nguyen MH, Lee S-J, Kriven WM. Synthesis of oxide powders by way of a polymeric steric entrapment precursor route. *J Mater Res* 1999, **14**: 3417–3426.
[19] Gülgün MA, Nguyen MH, Kriven WM. Polymerized organic-inorganic synthesis of mixed oxides. *J Am Ceram Soc* 1999, **82**: 556–560.
[20] Li Z-C, Zhang H, Bergman B, *et al*. Synthesis and characterization of $La_{0.85}Sr_{0.15}Ga_{0.85}Mg_{0.15}O_{3-\delta}$ electrolyte by steric entrapment synthesis method. *J Eur Ceram Soc* 2006, **26**: 2357–2364.
[21] Zhai Y, Ye C, Xia F, *et al*. Preparation of $La_{0.8}Sr_{0.2}Ga_{0.83}Mg_{0.17}O_{2.815}$ powders by microwave-induced poly(vinyl alcohol) solution polymerization. *J Power Sources* 2006, **162**: 146–150.
[22] Holland TJB, Redfern SAT. A nonlinear least-squares program for cell-parameter refinement implementing regression and deletion diagnostics. *J Appl Cryst* 1997, **30**: 84–85.
[23] Datta P, Majewski P, Aldinger F. Structural studies of Sr- and Mg-doped $LaGaO_3$. *J Alloys Compd* 2007, **438**: 232–237.
[24] Stevenson JW, Armstrong TR, Pederson LR, *et al*. Effect of A-site cation nonstoichiometry on the properties of doped lanthanum gallate. *Solid State Ionics* 1998, **113–115**: 571–583.
[25] Macdonald JR. *Impedance Spectroscopy: Emphasizing Solid Materials and Systems*. New York: Wiley Inc., 1987.